Crystalline Indole at High Pressure: Chemical Stability, Electronic, and Vibrational Properties

Margherita Citroni,* Barbara Costantini, Roberto Bini, and Vincenzo Schettino

LENS - European Laboratory for Nonlinear Spectroscopy, Universitá di Firenze, via N. Carrara 1, I-50019 Sesto F.no (FI), Italy, and Dipartimento di Chimica dell' Universitá di Firenze, via della Lastruccia 3, I-50019 Sesto F.no (FI), Italy

Received: July 28, 2009; Revised Manuscript Received: August 26, 2009

Vibrational and electronic spectra of crystalline indole were measured up to 25.5 GPa at room temperature in a diamond anvil cell. In particular, Fourier transform infrared (FTIR) spectra in the mid-infrared region and two-photon excitation profiles and fluorescence spectra in the region of the HOMO−LUMO transitions were obtained. The analysis of the FTIR spectra revealed a large red-shift of the N−H stretching mode with increasing pressure, indicating the strengthening of the H-bond between the NH group and the π electron density of nearest neighbor molecules. The frequencies of four vibronic bands belonging to the ^1L_a and ^1L_b systems were obtained as a function of pressure. Comparison with literature data shows that the crystal acts as a highly polar environment with regard to the position of the ^1L_b origin and of the fluorescence maximum, which are largely red-shifted with respect to the gas phase or to solutions in apolar solvents. A large, and increasing with pressure, frequency difference between the ^1L_b origin and the blue edge of the fluorescence spectrum suggests that the emitting state is ^1L_a, that is known to be more stabilized than ^1L_b by dipolar relaxation. Crystalline indole was found to be very stable with respect to pressure-induced reactivity. Only traces of a reaction product, containing saturated C−H bonds, are detected after a full compression−decompression cycle. In addition, differently from many unsaturated compounds at high pressure, irradiation with light matching a two-photon absorption for a HOMO−LUMO transition has no enhancing effect on reactivity. The chemical stability of indole at high pressure is ascribed to the crystal structure, where nearest neighbor molecules, formig H-bonds, are not in a favorable position to react, while reaction between equivalent molecules, for which a superposition of the π electron clouds would be possible, is hindered by H-bonded molecules. Consistently, no excimer emission was observed except at the cell opening at the end of the compression−decompression run. Extremely limited chemical reactivity and excimer formation likely occur at crystal defects, evidencing the strict connection between the two phenomena.

1. Introduction

Indole is an important biomolecule, being the fundamental constituent of the amino acid tryptophan and of many biologically important alkaloids. As a basic constituent of biologically significant molecules, and as a molecule of a size still compatible with ab initio calculations, it has been the subject of a considerable amount of spectroscopic measurements[1−26] and calculations.[3,19,27−32] In particular, the fluorescence of indole has been largely investigated, the absorption and fluorescence spectrum of tryptophan in the near UV region being due to transitions localized on the indole moiety. Tryptophan fluorescence is widely used to study protein structures and dynamics, being strongly sensitive to the polarity of the environment with regard to its intensity, lifetime, anisotropy, band shape, and wavelength of the maximum.[35−38]

An investigation of the effect of pressure on the vibrational and near UV spectra of crystalline indole is essential for the knowledge of the intermolecular interactions and their effects on the molecular geometries, the electronic distributions, and, ultimately, the chemical stability. Indeed, the application of static pressure allows a fine-tuning of the intermolecular distances, without changing the temperature and composition of the system. This may have important applications in the study of biological systems at high pressure.[39−41] Moreover, the application of pressure to molecular systems is known to produce both reversible and irreversible changes of the covalent bonds,[42,43] when the intermolecular distances are sufficiently reduced. High-pressure chemistry may be very selective and may give unexpected products due to the constraints by which molecules are bound in the high-density phases: the high viscosity in liquids and the relative orientations and distances in crystals. Probing the chemical stability of indole at high pressure would give an important piece of information in the context of high-pressure chemistry, since its molecular structure has similarities with aromatic systems that react extensively in the solid phase at high pressure. Benzene reacts at 40 GPa from annealed pure phase II crystals producing an amorphous hydrogenated carbon,[44,45] and heteroaromatic molecules like thiophene[46] and furan[47] react at 16 and at 10−12 GPa, respectively, to give amorphous compounds. In several molecular systems, including those mentioned, the reaction threshold pressure is considerably lowered by the absorption of light matching the transitions to the excited molecular electronic states, the excitation being sometimes able to open new reaction channels.[48−52] These findings have supported the idea that high-pressure chemistry has character of photochemistry. In this hypothesis, a chemical reaction may proceed through the thermal population of

* Corresponding author. Phone: +390554572503. Fax: +390554572451. E-mail: margherita@lens.unifi.it.

10.1021/jp907169p CCC: $40.75
Published on Web 09/21/2009

electronically excited states, made possible by the pressure-induced modification of their relative energies.[53] Alternatively, a chemical reaction may take place in the electronic ground state at a distorted geometry, similar to the configuration of minimum energy of an excited state. Indeed, the excitation of benzene to the first electronic excited states at a sufficiently high pressure has been shown to produce excimers[54] which are believed to have the same geometry as the ground state dimeric precursors[45] of the pressure-induced chemical transformation, thus explaining the lowering of the reaction threshold pressure with laser irradiation.

We thus carried out a spectroscopic investigation of indole at high pressure up to 25 GPa, paying special attention to its chemical behavior in order to relate it to the molecular structure and the crystalline environment at high pressure. The pressure evolution of the vibrational spectrum, of the two-photon excitation profile, and of the two-photon-induced fluorescence spectrum of crystalline indole was studied in a diamond anvil cell (DAC). The chemical stability of crystalline indole was probed with and without laser irradiation. The results, interpreted on the basis of the present knowledge of high-pressure reactivity in the condensed phases, provide support to the hypothesis that pressure-induced chemical reactions in aromatic systems occur when a superposition of the π-electron densities allows the formation of precursors whose geometry is similar to that of the corresponding excimers forming under photochemical activation. Two-photon (TP) fluorescence excitation spectroscopy was used because it has the advantage over one-photon (OP) spectroscopy of using excitation wavelengths in the visible region, avoiding diamond absorption. Moreover, the small two-photon absorption cross section allows a more precise detection of the absorption onset, and minimizes the sample damage.

2. Experimental Methods

Pressures up to 25.5 GPa were achieved by the use of a membrane diamond anvil cell (MDAC), equipped with IIa type diamonds, selected to have a low fluorescence background. Rhenium gaskets were used in all of the experiments. The initial sample dimensions were about 50 μm in thickness and 150 or 200 μm in diameter. For each run, a fresh sample of indole ($\geq$99% pure from Sigma-Aldrich) was loaded as one or more monocrystalline slabs, with no pressure medium. Anyway, the samples rapidly became highly polycrystalline as the pressure was applied. In one IR experiment, a KBr pellet was formed into the sample chamber before loading the indole sample, that was then deposited on the pellet, thus realizing a polycrystalline film of about 5 μm thickness. This sample was used to study the most intense IR absorptions that were saturated using the 50 μm thick sample.

The IR spectra were recorded in the mid-IR region 600−5000 cm^{-1} with a spectral resolution of 1 cm^{-1}, using a Bruker IFS-120HR FTIR spectrometer modified to allow measurements in the MDAC with a remote control of the pressure and *in situ* measurement of the pressure.[55] In the IR experiments, the pressure was measured by the ruby fluorescence method. The ruby fluorescence was excited with the second harmonic of a cw Nd:Yag laser (532 nm). The laser power was kept as low as a few milliwatts in order to avoid unwanted photochemical processes in the sample.

TP excitation profiles and fluorescence spectra were measured by using as an excitation source an optical parametric generator (EKSPLA - PG401) pumped by the third harmonic (355 nm) of a mode-locked Nd:Yag laser (EKSPLA - PL2143A) with a pulse duration of about 20 ps and a repetition rate of 10 Hz. Incident energies lower than 800 nJ per pulse were focused on the sample by using an achromatic doublet with a focal length of 75 mm. Before focalization, about 3% of the beam energy was reflected onto a fast UV-enhanced Si photodiode (Hamamatsu, S1722-02) for signal normalization. Emission from the sample was collected in backscattering geometry and analyzed by a single stage 1/4 m monochromator (2400 grooves per mm), coupled to a photomultiplier tube (ET-9235QB). Colored-glass filters (UG11 or BG3) were used to cut the residual excitation beam. The fluorescence spectra were obtained with a monochromator resolution of about 1 nm. The spectral resolution of the excitation profiles is limited in this experiment by the amplitude of the tuning steps of the PG, that was set to 1 nm. These conditions were chosen because the spectra did not reveal narrower lines at higher resolution. An oscilloscope (LeCroy LC584A) collects the signals from the PMT and from the reference photodiode. For each data point, both signals were averaged over 150 laser pulses and the average integrated areas and amplitudes were recorded. The quadratic dependence of the sample emission intensity on the excitation energy, indicating a two-photon absorption mechanism, was always checked before and after all of the measured spectra. Each data point in the reported spectra is the ratio of the integrated area of the average PMT signal to the square of the amplitude of the average photodiode signal.

For the measurement of the excitation profiles and emission spectra, all of the samples were loaded without ruby chips, to avoid any ruby fluorescence background and a possible sample heating due to absorption from the ruby. The pressure was indirectly measured recording the FTIR spectrum before and after any excitation or emission spectrum and comparing the IR absorption frequencies with those measured in the IR experiments, which thus served also as pressure-calibration runs. In particular, the pressure dependence of the ν_8, ν_9, ν_{16}, and ν_{31} modes was used. Room pressure measurements of the excitation profiles and fluorescence spectra were performed on polycrystalline ground samples in a quartz cuvette.

Optical catalysis of the chemical reaction of indole was probed using the 568 and 647 nm lines of a cw Kr^+ laser and the 514 nm line of a cw Ar^+ laser, with powers ranging from 50 to 600 mW. A lens having a focal length of 200 mm was used to focus the laser beam onto the sample, but the distance from the lens to the sample was chosen so that the whole sample (but not the gasket) was irradiated. Irradiation cycles were performed with time durations ranging from 2 to 6.5 h, at different pressures from 11.5 to 23.2 GPa.

3. Background

The vibrational spectrum of indole at room pressure has been analyzed in the gas, liquid, and solid phases and in solutions.[1−4,27,28] The indole molecule is planar (C_s symmetry) if the N−H bond is not considered. An increasingly strong red-shift, accompanied by a band broadening, of the N−H stretching mode was observed with respect to the gas phase on increasing the indole density (in CCl_4 solutions, in the liquid, in crystals at 10 and −180 °C).[1] This result was interpreted as due to the strengthening of an H-bond involving the NH moiety.

The crystal structure of indole[5] at room pressure is orthorhombic $Pna2_1$ (C_{2v}^9) with 4 molecules per unit cell (a = 7.86 Å, b = 5.66 Å, c = 14.89 Å). Refinement of the atomic positions (not including H atoms) showed that the L molecular axis is parallel to the c crystallographic axis (Figure 1). The minimum intermolecular distance (3.38 Å) occurs between the N and the C3 atoms of nearest neighbor molecules along a direction

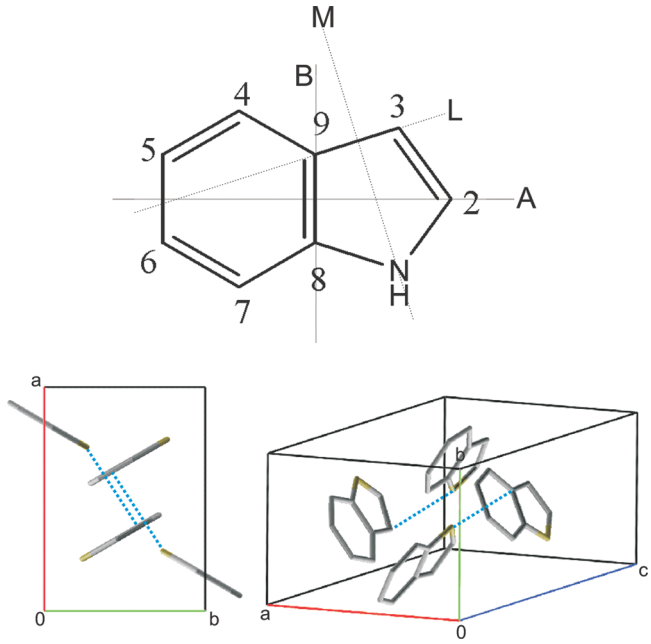

Figure 1. The indole molecule and two views of the unit cell of the indole crystal as reported in ref 5. A is the long molecular axis, laying in the molecular plane and analogue of the C_2 symmetry axis of the parent 9-annulene anion; B is the short molecular axis, laying in the molecular plane and perpendicular to A. The L and M molecular axes are defined in ref 13. Dotted lines in the crystal indicate the shortest intermolecular distance (3.38 Å).

approximately laying in the (110) plane and with its major component along *a*. This is consistent with H-bonding between the NH moiety and the π electron distribution of the nearest neighbor molecule, developing along this direction.

The absorption spectrum of indole in the range 290−220 nm is dominated by the spin and symmetry allowed $\pi \rightarrow \pi^*$ HOMO−LUMO transitions to four states named ^1L_a, ^1L_b, ^1B_a, and ^1B_b in analogy with Platt's notation for aromatic hydrocarbons.[33] Transitions to the ^1B states are fully allowed, while transitions to the ^1L states are forbidden by the selection rule $\Delta k = \pm 1$, where k is the quantum number related to the out of plane component of the electron orbital angular momentum, and thus much weaker.[34] In indole, the large overlap of the vibronic transitions to the two ^1L states and the strong dependence of the absorption and fluorescence spectra on the experimental conditions (phase, solvent, temperature) make the exact location of these two states, especially ^1L_a, and the identification of the emitting state in different environments particularly tricky. In the gas phase, the lowest energy transition is $^1A \rightarrow {}^1L_b$, whose origin is at 283.8 nm,[6,7] while the ^1L_a origin has been located 1400 cm^{-1} above the ^1L_b origin.[8] Both $^1A \rightarrow {}^1L_b$ and $^1A \rightarrow {}^1L_a$ transition moments[9,10] lay in the molecular plane, at right angles to each other, and spectral ranges with the predominance of transitions involving either ^1L_b or ^1L_a have been distinguished by polarization measurements.[11−14] Alternatively, they have been distinguished by their different solvatochromism.[15−17] In fact, the energy of the $^1A \rightarrow {}^1L_a$ transition is much more sensitive to the environment than the energy of $^1A \rightarrow {}^1L_b$, undergoing a stronger red-shift with increasing solvent polarity. This has been ascribed to the formation of ground state indole−solvent complexes.[16,18,19]

Particularly significant is the dependence of the fluorescence spectrum upon the solvent polarity. It has been demonstrated by the measurement of solvatochromic shifts that when the solvent polarity is increased there is a change in the emitting state from ^1L_b to ^1L_a,[16,17] due to solvent relaxation around the excited molecule in the ^1L_a state.[16,20] Indeed, the ^1L_a state in its relaxed geometry has a much larger dipole moment (about 6 D) than both the ^1A and ^1L_b states (about 2 D).[21,22,29−32] Recent calculations[23] show that in aqueous solution optical population of either ^1L_b or ^1L_a is followed by the lowering in energy of ^1L_a through solvent relaxation, so that ^1L_a is the emitting state.

To our knowledge, there is no fluorescence spectrum of crystalline indole in the literature, while absorption spectra of single crystals of indole have been performed with polarized light.[12,13] The existence of two different absorption systems having different polarization directions has been reported (the observed frequencies and their assigments are listed in Table 1). The lowest energy absorption system (^1L_b) is found to be polarized along the M molecular axis, while the highest energy absorption (^1L_a) is polarized along the L molecular axis.[13]

The only available information about the spectroscopy of indole as a function of pressure concerns the emission of indole in solutions.[24−26] In particular, the location of the fluorescence and phosphorescence maxima and the fluorescence and phosphorescence quantum yields and lifetimes were studied up to 12 GPa in 10^{-2} M solutions in PMMA. Both the fluorescence and phosphorescence maxima red-shift with pressure, but the pressure shift of the phosphorescence maximum has a smaller slope. This means that the energies of S_0, S_1, and T_1 increase at different rates and S_1 and T_1 get closer with increasing pressure. Through this mechanism, the pressure increases the rate of intersystem crossing; in fact, an increase in the phosphorescence intensity was observed on compression.

4. Results

4.1. Infrared Spectra. The mid-infrared absorption spectra measured below 1 GPa (Figure 2) nicely agree with the vibrational spectra reported by previous authors at room pressure.[1−4] Indole (C_s symmetry if the N−H bond is neglected) has 42 normal modes: 29 in plane (a′) and 13 out of plane (a″), all IR and Raman active. Several modes were classifed by Lautié et al.[1] as vibrations mainly involving either the benzene ring (denoted by ϕ and numbered with the Wilson notation for benzene[56]) or the pyrrole ring (denoted by π and numbered with the Lord and Miller notation for pyrrole[57]). Each internal mode splits in the crystal into four components, three of which are IR active. The vibrational modes in the present work are numbered following ref 3. In Table 2, we report the assignment of the modes from ref 1, in general agreement with ref 3.

The pressure was increased up to 25.5 GPa in steps of 0.5−1 GPa, and a FTIR spectrum was measured at each step after pressure stabilization. A selection of the measured spectra is shown in Figure 2. All of the absorption bands broaden and blue-shift with increasing pressure, except those assigned to the N−H stretching mode ν_1, that undergo a red-shift. In Figure 3, we show the pressure dependence of the frequencies of the most intense components of several modes assigned to vibrations mainly involving either the benzene or the pyrrole ring.[1,3] For all of the observed modes, we note that in the range 3−8 GPa those assigned to vibrations of the benzene ring have generally a more linear pressure shift than those assigned to vibrations of the pyrrole moiety. Specifically, the pressure shift of the pyrrole modes presents a slope change between 3.5 and 7 GPa, this being particularly evident for the ν_{21} mode. Most bands intensify with increasing pressure: ν_{31}, ν_{16}, ν_{14}, ν_{12}, ν_{11}, and ν_9, all assigned to the benzene ring, all the C−H stretching modes (localized either on the benzene or on the pyrrole ring) and the N−H stretching mode ν_1. In particular, the intensity of the ν_2

TABLE 1: Peak Frequencies (cm^{-1}) and Assignments of the UV Absorptions of Crystalline Indole

1 bar (ref 12)	1 bar (ref 13)	assignment (ref 13)	1 bar (this work)	0.5 GPa (this work)	1 bar[a] (ref 15)	assignment (ref 15)
34500/34250	34540/34443	0−0 ^1L_b	34560	34501	34734, s	0−0 ^1L_b
					35150, m	0−0 ^1L_a
					35262, w	0 + 530 ^1L_b
35350/35100	35340/35240	0 + 800/797 ^1L_b	35236	35267	35461, s	0 + 730 ^1L_b
					35638, m	0 + 900 ^1L_b
					35727, m	0 + 990 ^1L_b
	35725/35625	0 + 1185/1182 ^1L_b	35997	35951	36050, m	0 + 1310 ^1L_b
					36166, m	0 + 1000 ^1L_a
					36430, m	0 + 1690 ^1L_b?
36650/∼36675	∼37000	^1L_a	36928	36955	36900, m	0 + 1750 ^1L_a
					37594, m	0 + 2450 ^1L_a

[a] Indole in cyclohexane solution at −196 °C.

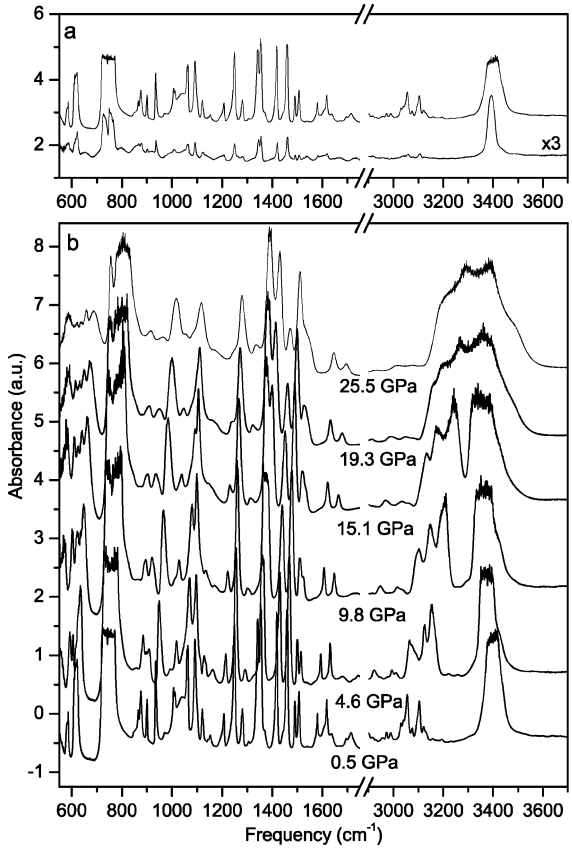

Figure 2. Panel a: FTIR spectra of polycrystalline indole at low pressure. Upper trace: massive sample (50 μm thick) at 0.5 GPa. Lower trace: thin sample (about 5 μm thick) deposited on a KBr pellet, at 0.95 GPa. Panel b: FTIR spectra of polycrystalline indole (massive sample) at selected pressures on compression.

mode (mainly a C2−H stretching) grows much faster than all of the other C−H stretching modes: initially, the less intense, it exceeds the intensity of all the other CH stretching modes above 6 GPa. On the other hand, ν_{36}, ν_{33}, ν_{24}, ν_{18}, ν_{15}, ν_{13}, and ν_{10}, all assigned to the pyrrole ring, as well as ν_8, weaken with pressure.

The pressure was released measuring FTIR spectra in steps of about 5 GPa on the massive sample and in steps of about 1 GPa on the 5 μm thick sample. All of the frequencies, bandwidths, and relative intensities of the indole absorption bands are fully reversible with pressure. Anyway, the overall intensity of the indole absorptions slightly decreases on decompression, while a broadband grows around 2920 cm^{-1}. In Figure 4, the spectrum of a massive indole sample after the loading is compared to the last spectrum of the decompression run and the difference spectrum is shown. Difference spectra were obtained subtracting from each spectrum measured on decompression a spectrum measured on compression at the same pressure. The new band, assigned to C−H stretching modes involving C atoms with sp^3 hybridization, indicates the opening of the aromatic indole ring. This band was fitted to a convolution of pseudo-Voigt functions, and the total integrated area is reported as a function of pressure in the inset of Figure 4. This shows that the reactive process mainly occurs as the pressure is released, especially near room pressure. The datum at 19.6 GPa is underestimated because the new band is already present, although very weak, at this pressure upon compression. We can thus locate the threshold pressure for this chemical reaction approximately between 15 and 20 GPa on compression.

4.2. Two-Photon Fluorescence and Excitation Profiles. Two-photon fluorescence spectra and the corresponding excitation profiles were measured in the DAC as a function of pressure up to 20.8 GPa in steps of 1−2 GPa. FTIR spectra were recorded at each pressure step before and after the measurement of the TP spectrum to determine the pressure as described in the Experimental Methods section, and to accurately check if any chemical reaction had occurred. Moreover, the sample was visually observed at the microscope before and after each measurement to verify that it had not been damaged by the laser radiation.

For each pressure step, two or more fluorescence spectra were measured, in the range 300−450 nm, using different two-photon excitation wavelengths. No differences were found, indicating that fluorescence occurs from a thermally relaxed excited state. The fluorescence spectrum undergoes a red-shift with pressure and its intensity decreases, as reported for indole solutions in PMMA.[24] Some fluorescence spectra measured on increasing pressures are shown in Figure 5. All of the fluorescence spectra were reproduced by a convolution of pseudo-Voigt functions. A minimum of four (below 4 GPa) or five (above 4 GPa) bands were necessary for the fit, and their peak frequencies are reported as a function of pressure in Figure 6. An additional peak was used to reproduce the signal of the 355 nm light from the pump laser that reached the PMT tube. The pressure shift of all the peak frequencies is nearly linear, with an average $d\nu/dP$ value of −250 cm^{-1}/GPa. The frequencies are reversible with pressure with some hysteresis, as shown by the blue symbols of Figure 6. The last step of decompression (from 3.0 to 0.8 GPa) caused a major change in the emission spectrum, consisting of the sudden appearance of a new band red-shifted by about 4800−5000 cm^{-1} with respect to the most intense peak of the indole fluorescence. This broad and weak band is likely to ascribe to the formation of excimers at crystal defects, as explained in the Discussion section. It is also possible that this

TABLE 2: Band Frequencies (cm^{-1}) and Assignments of the Vibrational Modes of Crystalline Indole[a]

0.95 GPa[b] (this work)	0.5 GPa[c] (this work)	1 bar[d] (ref 3)	1 bar (liquid)[e] (ref 1)	1 bar[f] (ref 4)	mode (ref 3)	type (ref 3)	description (ref 1)
582, 588	579, 583, 586	576	575	578	ν_{38}	a″	R″
610, 615, 622	610, 616, 622	609	607	608, 619s	ν_{27}	a′	R′ϕ (ref 3: R′)
		607	608		ν_{37}	a″	R″(ref 3: R″π)
725, 737	saturated	721	725		ν_{36}	a″	γCHπ on C3
750, 756		743	743	730	ν_{35}	a″	γCHϕ (11)
764, 770		760	758	758	ν_{26}	a′	R′ϕ breathing (1)
		767	767		ν_{34}	a″	R′π[g]
	849	849	848	854	ν_{33}	a″	γCHπ on C2
878	875	877	873	867	ν_{25}	a′	γCHϕ[h]
899, 902	898, 901	896	895	898	ν_{24}	a′	R′π breathing
935, 940	934, 938	934	930	937	ν_{31}	a″	γCHϕ (17b)
	971	971	970	971	ν_{30}	a″	γCHϕ (5)
1008, 1014	1007, 1012	1008	1010	1006	ν_{23}	a′	δCHϕ (18b)
1062, 1065	1060, 1064	1060	1064	1059	ν_{22}	a′	δCHπ on C3
1092, 1101	1091, 1100	1095	1092		ν_{21}	a′	δCHπ on C2
1122	1121	1119	1119		ν_{20}	a′	δCHϕ (9b)
	1145, 1153	1152	1147		ν_{19}	a′	δNH[i]
1208	1198, 1204, **1207**	1205	1203	1198	ν_{18}	a′	R′π
1243, **1250**	1242, **1249**	1248	1245	1249	ν_{16}	a′	δCHϕ (3)
1282	1276, **1281**, 1284	1278	1276	1282	ν_{15}	a′	R′π (5)
1339, **1346**, **1355**	1335, **1342**, **1355**, 1370	1338, 1353	1334, 1352	1348	ν_{14}	a′	R′ϕ (14), R′π (14)[j]
1416, **1420**	1407, 1413, **1418**	1415	1412	1414	ν_{13}	a′	R′π (6)
1461	1443, 1453, **1459**	1455	1455	1461	ν_{12}	a′	R′ϕ (19b)
1491	1490	1487	1487		ν_{11}	a′	R′ϕ (19a)
1507	1503, **1507**	1506	1509	1496	ν_{10}	a′	R′π (15)
1573, **1581**, 1594	1573, **1580**, 1591	1578	1576		ν_{9}	a′	R′ϕ (8b)
1608, **1619**	1607, **1617**	1616	1616	1601	ν_{8}	a′	R′ϕ (8a)
3034, 3044, 3059, 3078	3030, 3039, 3047, 3056, 3075	3024			ν_{7}	a′	νCHϕ
		3047			ν_{5}	a′	νCHϕ
		3055			ν_{6}	a′	νCHϕ
		3062			ν_{4}	a′	νCHϕ
3105	3095, **3104**	3101			ν_{3}	a′	νCHπ mainly on C3
3123, 3133	**3121**, 3131	3122			ν_{2}	a′	νCHπ mainly on C2
3382, **3397**	saturated	3398	3418		ν_{1}	a′	νNH

[a] The boldface characters indicate the most intense peaks in the Davydov multiplets. [b] Thin film, IR. [c] Massive sample, IR. [d] Raman. [e] 70 °C, IR. [f] Inelastic neutron scattering. [g] Assigned as a″ in ref 3 and a′ in ref 1. [h] Assigned as a′ in ref 3 and a″ in refs 4 and 1. [i] Assigned as R′ in ref 3. [j] In ref 3, the two peaks at 1338 and 1353 cm^{-1} are assigned to the mode ν_{14}, in plane CH and skeletal bending mainly localized on the pyrrole ring; in ref 1, the two bands at 1334 and 1352 cm^{-1} are assigned to two distinct modes, in plane skeletal vibrations localized on the benzene and on the pyrrole ring, respectively.

emission is due to the small amount of reaction product that forms when the pressure is completely released.

The excitation profiles were measured in the range 450−620 nm, using the maximum of the fluorescence signal (black circles in Figure 6). The relative intensities of the absorption bands were found to depend on the crystal orientation. An example of this effect is given in the left panel of Figure 7. Nevertheless, since the diameter of the focused beam on the sample was about 25 μm, and the average diameter of a single crystal was smaller, we are not able to select a single orientation because we are generally probing more than one crystallite. For our measurements, we decided to always choose a sample region and rotation angle of the DAC that maximized the intensity of the lowest frequecy peak, in order to have consistent data to follow the evolution of the electronic spectrum with pressure. Some excitation profiles at different pressures are shown in Figure 8. The peaks in the low-frequency range (600−530 nm at the lowest pressures) correspond to vibronic transitions to the ^1L_a and ^1L_b states, while the steep intensity increase in the high-frequency range represents the red edge of the fully allowed transitions to the ^1B states. The bands broaden and red-shift with rising pressure. The absorptions due to the trasitions to ^1B_a and ^1B_b overlap those to the lower energy states above 5 GPa (see Figure 8). This could result from a faster red-shift with pressure of these high-energy bands or, more likely, to their broadening or intensification with pressure. The overall intensity of the excitation profile decreases with pressure due to the decrease in the fluorescence quantum yield. The excitation profiles in the region of the $^1A \rightarrow {}^1L_b$ and $^1A \rightarrow {}^1L_a$ transitions were analyzed by deconvolution with pseudo-Voigt functions after subtraction of the background signal due to transitions to the higher frequency ^1B states. At the lower pressures, a minimum of four peaks was necessary to accurately reproduce the spectrum; above 5 GPa, only three peaks were employed. These peaks can be correlated to the one-photon absorption bands observed in single crystals in refs 12 and 13, as reported in Table 1. The pressure evolution of their frequencies is shown in Figure 6. The average shift $d\nu/dP$ of the observed absorption peaks is -160 cm^{-1}/GPa. The excitation profile is reversible with pressure, in bandwidths, frequencies, and intensities, with no hysteresis, and after the compression−decompression cycle, the same low-pressure excitation profile is obtained.

4.3. Probing the Optical Catalysis. On a fresh sample of crystalline indole, 50 μm thick, the pressure was slowly increased and irradiation cycles were performed using wavelengths that are absorbed through a two-photon process, as reported in Table 3. Before and after each cycle, an FTIR spectrum was measured, and a difference spectrum was

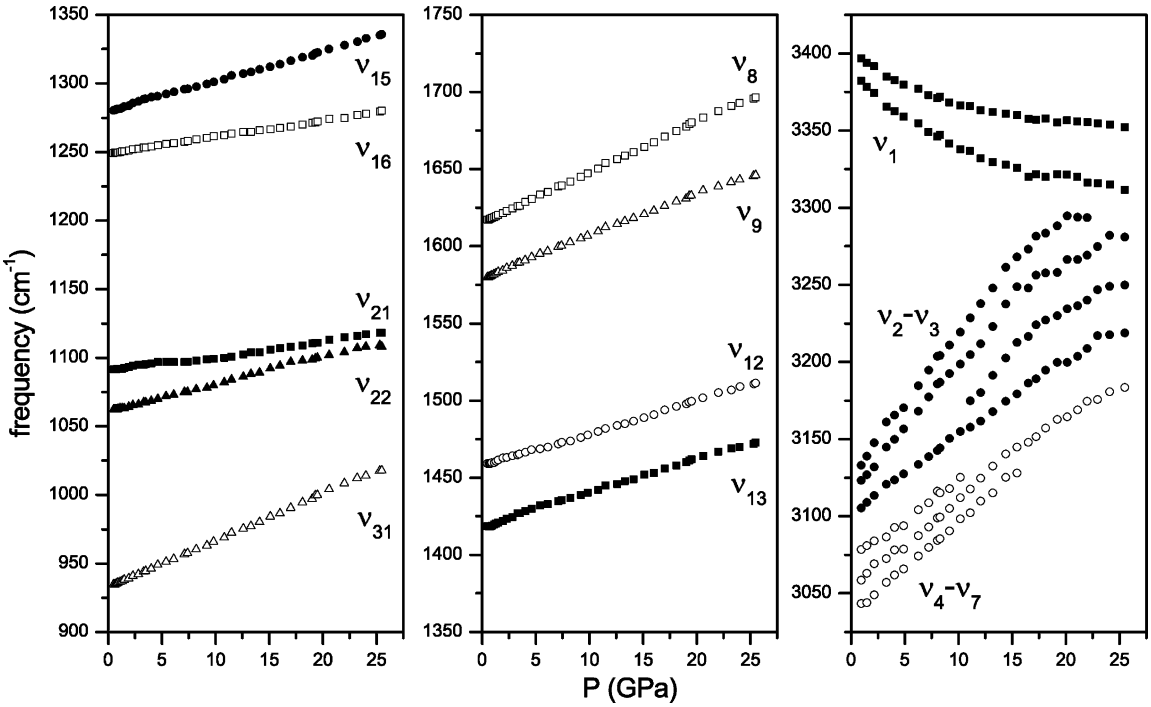

Figure 3. Frequency vs pressure evolution of some IR absorption bands. Full and empty symbols represent modes assigned to vibrations mainly involving the pyrrole and the benzene ring, respectively.[1,3]

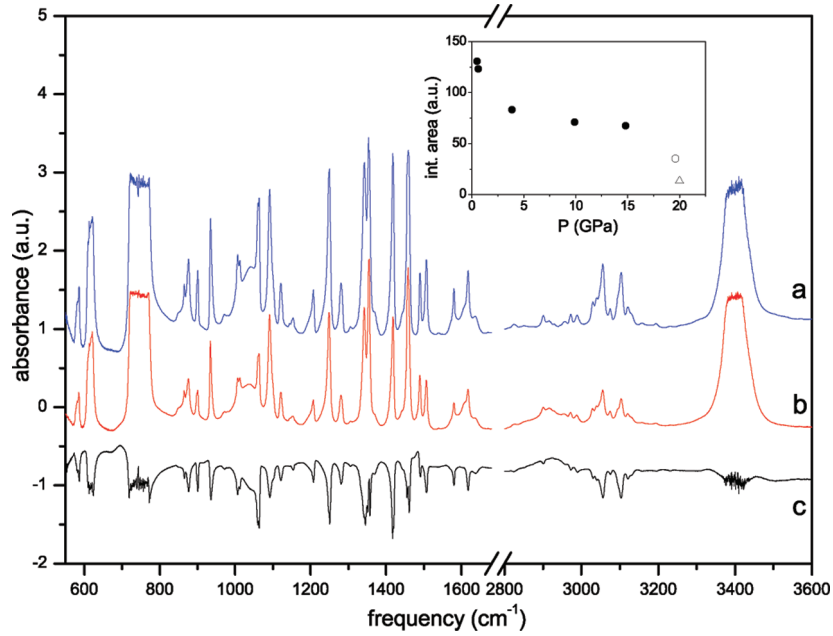

Figure 4. FTIR spectra of polycrystalline indole (massive sample) in the DAC at 0.5 GPa on compression (a) and decompression (b). Trace c is the difference spectrum. In the inset, the integrated area of the new sp^3 CH stretching band is reported as a function of pressure on decompression. Circles: data from difference spectra (difference between spectrum on decompression and spectrum on compression at a given pressure). The empty circle at 19.4 GPa represents an underestimation of the real integrated area of the new band, due to the presence of a weak absorption also in the spectrum measured on compression. Empty triangle: datum from the difference spectrum between the spectra measured after and before irradiation with the 514 nm line of an Ar^+ laser of a sample at 20.0 GPa.

calculated, to check whether any new band had appeared or the indole absorptions had weakened. Only after the cycle number 5 (see table) performed at 20 GPa, the apperance of the same sp^3 CH stretching band as in the purely pressure-induced chemical reaction was detected. Further irradiation at the same or higher pressure had no effect. In contrast to the purely pressure-induced reaction, the sp^3 CH stretching absorption did not grow in intensity on decompression. The spectrum measured at the lowest pressure shows that the quantity of product is comparable or even less than in the purely pressure-induced process. We cannot prove that the same product is formed in the two processes, because we can only rely on the weak broadband due to C−H stretching modes involving sp^3 C atoms, that is a not very diagnostic spectral region, and on the weakening of the indole absorption bands.

5. Discussion

The spectroscopic data obtained in this work outline a pronounced chemical and photochemical stability of indole up

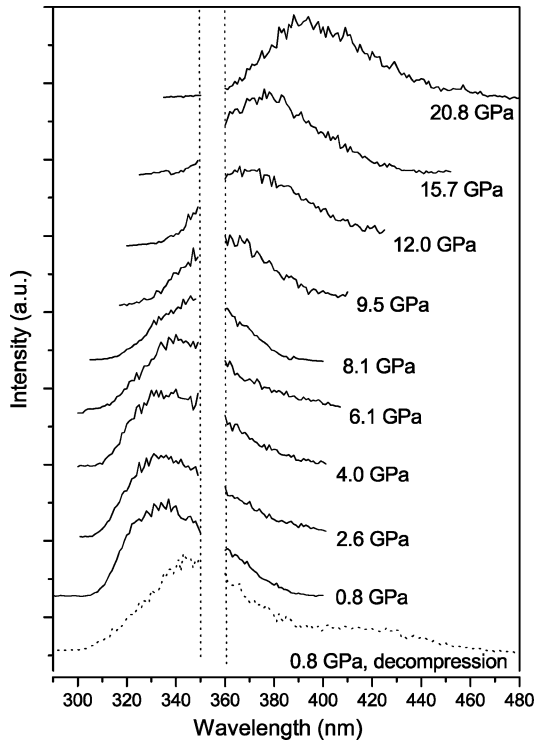

Figure 5. Two-photon fluorescence spectra measured at selected pressures on compression. The dotted trace is the two-photon fluorescence spectrum measured at 0.8 GPa on decompression. The frequency range 350−360 nm is not reported, as it contains the residual signal deriving from the pump laser at 355 nm.

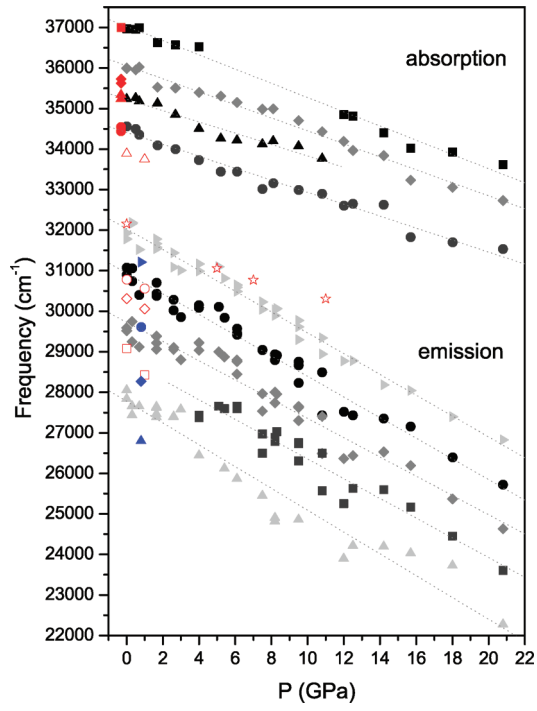

Figure 6. Black and gray symbols: pressure evolution of the peak frequecies obtained from the deconvolution of the two-photon excitation and fluorescence spectra measured upon compression. The emission maximum corresponds to the black circles. The dotted lines indicate the linear fit of the data for each observed peak. Blue symbols: fluorescence peak frequencies in the last step of decompression. Full red symbols: absorption peak frequencies in single crystals at room pressure from refs 12 and 13. Empty red symbols: values of the fluorescence maximum reported in refs 24 and 25 for indole in different solvents up to 1 GPa. Triangles: hexane. Stars: PMMA. Circles: glycerol, propanol, butanol. Diamonds: methanol. Squares: water.

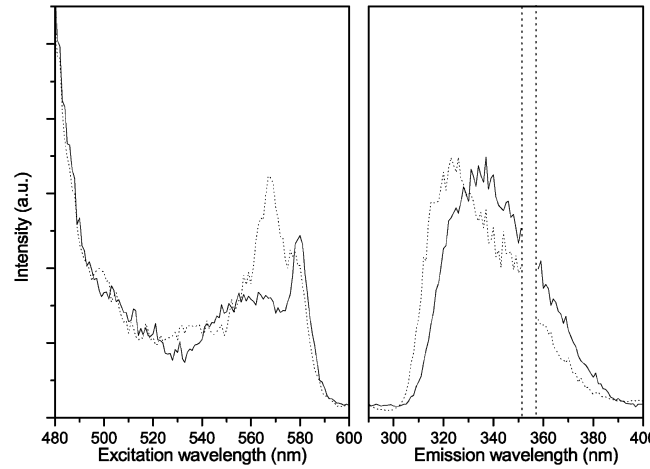

Figure 7. Low-pressure excitation (left panel) and fluorescence (right panel) spectra of crystalline indole at room pressure (dotted line) and at 0.5 GPa (solid line). The comparison between the two excitation profiles (left panel) shows the effect of the sample orientation with respect to the excitation beam. The comparison between the two fluorescence spectra (right panel) shows the large pressure shift of the emission spectrum.

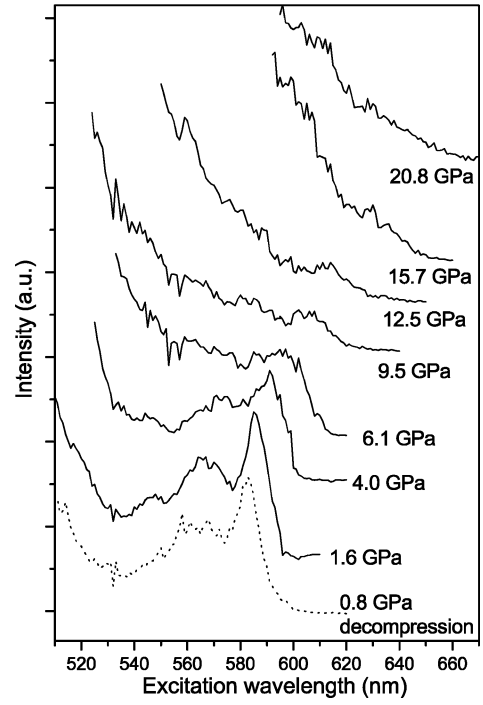

Figure 8. Solid traces: two-photon excitation profiles at selected pressures on compression. Dotted trace: two-photon excitation profile at 0.8 GPa after decompression.

to considerably high pressures despite the presence of a heteroatom, which is known to enhance reactivity in other aromatic systems.[46,47]

The analysis of the IR spectra shows that all of the vibrational modes undergo a blue-shift with pressure, as is usually observed in molecular systems, because of the stiffening of the structure with increasing density. The only exception is represented by the N−H stretching mode (ν_1) that undergoes a large red-shift. The value of 3352 cm^{-1} of the NH stretching frequency at 25.1 GPa, compared to 3397 cm^{-1} at 0.95 GPa, means a 3% reduction of the force constant of the N−H bond. As already mentioned, the softening of this mode has been observed by Lautié et al.[1] with increasing density of the system from vapor to liquid to

TABLE 3: Parameters of the Irradiation Cycles Performed to Probe the Stability of Indole under Photoirradiation

n	*P* (GPa)	duration (min)	power (mW)	λ (nm)	final state[a]
1	11.5	220	50	568	^1L_a, ^1L_b
2	12.6	130	135	514	^1B_a, ^1B_b
3	16.8	120	130	514	^1B_a, ^1B_b
4	16.8	130	500	514	^1B_a, ^1B_b
5	20.0	120	150	514	^1B_a, ^1B_b
6	20.0	120	350	514	^1B_a, ^1B_b
7	20.0	180	600	514	^1B_a, ^1B_b
8	20.0	390	600	514	^1B_a, ^1B_b
9	23.2	335	530	514	^1B_a, ^1B_b
10	24.0	420	535	647	edge of ^1L_b

[a] Excited states reached by two-photon absorption.

solid and lowering the temperature, and was attributed to the formation of a H-bond involving the NH moiety. The crystal structure[5] allows the formation of N−H···π bonds, with a minimum intermolecular distance of 3.38 Å at room pressure, between N and C3 of nearest neighbor molecules. The pyrrole part of the heteroaromatic bicyclic structure is thus more involved than the benzene ring in the interaction, both as a H-bond donor (the NH moiety) and as a H-bond acceptor (the π electrons). The considerable red-shift of ν_1 that we observe on increasing pressure indicates that this H-bond gets stronger with pressure. The pressure evolution of the infrared spectrum can also provide some additional hints on the response of the crystal structure to the increasing density. The less regular hardening and the intensity decrease of several pyrrole modes, and the strong intensification of the C2−H stretching mode ν_2, along with the red-shift and intensification of ν_1, suggest that the geometry of the pyrrole ring is more affected than that of the benzene ring on compression. Moreover, the difference in the pressure evolution of the frequencies of two very similar vibrational modes: ν_{21} (mainly C2−H in plane bending) and ν_{22} (mainly C3−H in plane bending), indicates a difference in the compressibilities of the C2 and C3 positions. In particular, the vibration in the C2 position undergoes a smaller blue-shift and two slope changes, at 3.5 and 7 GPa. It is interesting to note that at 3.5 GPa also the intensity inversion between the ν_2 (C2−H stretching) and ν_3 (C3−H stretching) occurs. This could indicate that while at room pressure the H-bond mainly involves the C3 position, at higher pressure the C2 atom becomes the closest contact to the nearest neighbor NH group, and is thus more involved in the H-bond than the C3 atom. In any case, the strengthening of the NH···π bonds is evidenced by the red-shift of ν_1, so that pressure causes the formation of long chains of H-bonded molecules, possibly distorted by an orientational disorder as suggested in ref 5. The buildup of these strong intermolecular interactions stabilizes a reciprocal orientation of molecules that is scarcely reactive. In fact, the π electron distributions of nearest neighbor molecules (see Figure 1) do not lay in parallel planes and cannot overlap efficiently to react. On the other hand, the interaction between equivalent molecules, which are in a favorable configuration for reactivity, is hindered by the presence of an H-bonded molecule. The IR spectrum is reversible with pressure except for the appearance of a very weak, broad band in the sp^3 C−H stretching region, indicating the opening of the aromatic system and the formation of saturated C−H bonds. The product mostly forms in decompression, as also observed in the pressure-induced reactivity of benzene.[44] This behavior can be ascribed to the positive activation volume of the reaction, which has at least one reorientational or bond cleavage step requiring an extra volume. Anyway in the case of indole the amount of product that is obtained when the pressure is completely released is negligible, suggesting that the reaction occurs only at specific points such as crystal defects. The geometry of the H-bond in the case of indole prevents high-pressure reactivity: this is not the case in other molecular crystals like nitromethane, where the formation of H-bonds at high pressure[58] preludes to the triggering of a complex reaction involving the entire crystal.[59,60]

Besides the vibrational properties, another rich source of information about the pressure-induced reactivity of aromatic compounds is the pressure evolution of the electronic properties. The missed observation of structural excimers at high pressure is fully consistent with the lack of an extended pressure-induced reactivity in the crystal. The appearance of a large unstructured band in the red part of the fluorescence spectrum, red-shifted by about 5000 cm^{-1} with respect to the monomer emission peak, is reported for several aromatic molecules at high pressure and ascribed to excimer emission.[54,61−64] The formation of excimers can be caused by the approach of properly oriented molecules at high density[54] or, more frequently, occurs at crystal defects that make possible an accidental favorable overlap of the π-electron densities.[61−64] The weak, broad emission band observed around 24000 cm^{-1} in the last spectrum after decompression is attributable to the formation of excimers, that may form at crystal defects because, as previously stated, the crystal structure of indole is unfavorable to excimer formation and to reactivity. These results nicely agree with the missed observation of a photochemical activation of the reaction. In fact, the small quantity of product formed under irradiation with no increase in yield on increasing or releasing pressure seems to confirm that the reaction only occurs at crystal defects.

The presssure behavior of the electronic excited states provides interesting hints on the photophysical properties and their changes with the density. In the fluorescence excitation profiles, we cannot assign with certainty the observed bands to ^1L_a or ^1L_b, but due to the close resemblance of our excitation profiles to the absorption spectra reported in the literature,[12,13] we can rely on their assigment. Therefore, the three lowest energy bands should belong to the ^1L_b system and the highest energy band to the ^1L_a system (see Table 1). Anyway, the difficulty of the assignment lies in the identification of the origin of the ^1L_a system, because the energy of the $^1A \rightarrow {}^1L_a$ transition is very sensitive to the sample conditions. At temperatures below −110 °C, aggregation phenomena in 2-methylpentane solutions are reported to broaden both the absorption and the fluorescence spectra with decreasing temperature, while the red part of the fluorescence spectrum is reported to intensify.[14] In the absorption spectrum in cyclohexane at −196 °C, the ^1L_b origin is at 287.9 nm and the ^1L_a origin is 416 cm^{-1} above it.[15] Adopting this assigmnent for our spectra, the lowest energy band is the ^1L_b origin, the following is a vibronic band of the ^1L_b system at about 700 cm^{-1}, the third one is the sum of two vibronic bands of the ^1L_b and one of ^1L_a system (it is predominantly ^1L_b), and the highest energy one is the sum of two vibronic bands of the ^1L_a system. Thus, the assigment coincides with that of refs 12 and 13 for the solid phase.

The analysis of the fluorescence spectra is also very interesting. The vibronic structure of the fluorescence spectrum in cyclohexane at −196 °C mirrors the absorption spectrum.[15] Our case is completely different; in fact, we find a larger Stokes shift, as reported for indole in polar solvents, and we also detect the highest energy fluorescence peak at a much lower frequency than the ^1L_b origin, by about 2650 cm^{-1} (see Figure 6). Catalan and Diaz[17] report the values of the ^1L_b origin in the absorption spectrum and of the emission maximum in many different

solvents and solvent mixtures. The value that we find for the ^1L_b origin at room pressure in the crystal (34560 cm^{-1}) corresponds to the most red-shifted value that they found (34583 cm^{-1}), of indole in dimethyl sulfoxide, the most polar solvent probed. Our emission maximum corresponds to the second peak in order of decreasing energy (black circles in Figure 6), and is at 30900 cm^{-1} at room pressure. This corresponds to the values of the fluorescence maximum found in highly polar solvents (dioxane/water, 1-butanol, ethanol, methanol, *N*-methylformamide, *N*,*N*-dimethylacetamide).[17] Moreover, if we compare the frequency of our emission maximum with those found below 1 GPa by Drickamer and co-workers[24,25] in several solvents, we find the maximum similarity with the values found for indole in polar solvents like glycerol, propanol, butanol, and methanol. Thus, the crystal seems to act like a polar solvent, as the frequencies of the ^1L_b origin and emission maximum are concerned. As mentioned in the Background section, it is known that in polar solvents emission occurs from ^1L_a, due to solvent relaxation that inverts the energies of ^1L_b and ^1L_a. The large frequency shift that we find betwen the origins of the excitation and fluorescence spectra could indicate that this energy inversion also occurs in crystalline indole. The slope of the pressure shift of the fluorescence bands is about twice that of the excitation profile peaks. In a two-state system (where emission occurs from the same state involved in the absorption process), the different pressure shift of the absorption and fluorescence spectra may be due to the different "horizontal shift" of the two electronic states, i.e., to a different displacement of the two minima with pressure, or alternatively to a different modification of the potential energy surfaces not necessarily involving a displacement of the minima. In both cases, emission occurs to vibrationally excited levels of the electronic ground state and thus at lower energy than absorption, so that the different compressibilities of the two electronic states are evidenced by the different pressure shifts of the absorption and fluorescence spectra. Moreover, a larger pressure red-shift of emission with respect to absorption can also be due to an increasingly strong stabilization of the emitting state by the dipole relaxation of the crystalline environment. In the case of indole, all of these effects can be active if the emitting state is either ^1L_b or ^1L_a, the latter being anyway much more sensitive to solvent relaxation due to its larger dipole moment.

6. Conclusions

A combined vibrational and electronic study was performed on crystalline indole up to 25.5 GPa, finalized to understand the structural and photophysical properties, and the chemical stability, of indole as a function of pressure. In particular, a large red-shift of the N−H stretching mode was observed in the IR spectra with raising pressure, indicating an increase in the strength of the NH$\cdots\pi$ H-bond. This interaction stabilizes a crystal structure where no overlap of the π-electron densities of adjacent molecules is allowed. Two-photon excitation profiles and fluorescence spectra were performed as a function of pressure up to 20.8 GPa, with excitation wavelengths in the range 450−620 nm. For the first time, information was obtained on the absorption in the spectral region of the HOMO−LUMO transitions and on the fluorescence spectrum of crystalline indole as a function of pressure. The crystalline environment was found to red-shift the absorption and fluorescence peaks with respect to the gas phase similarly to a highly polar solvent. The application of pressure further red-shifts absorption and emission. The slope of the peak frequencies as a function of pressure is about twice for fluorescence than for absorption, indicating a different compressibility for the ground and the emitting states, or an increased stabilization of the emitting state by dipole relaxation with increasing pressure. Our results are consistent with emission from either ^1L_b or ^1L_a, but the large, and increasing with pressure, frequency shift between the origins of the absorption and emission spectra give stronger support to the hypothesis that ^1L_a is the emitting state. No excimer emission was observed upon compression. Small traces of a reaction product, evidenced in the IR spectra by a weak broadband in the region of the sp^3-CH stretching absorptions, are observed at the end of each experiment, with not reproducible quantities or threshold pressures, indicating that reactivity occurs at crystal defects. A negligible amount of product is also observed when the sample is irradiated with a high-power cw laser in the regions of TP absorption, confirming the high stability of the crystal, where a chemical reaction can only take place at crystal defects. We can relate the chemical stability of indole with its crystal structure, stabilized by the strengthening of the H-bonds with pressure, that prevents the overlap of π-electron densities between molecules that could trigger a chemical reaction. Indeed, the failure to detect excimer emission at high pressure also indicates the lack of an efficient intermolecular overlap of π-electron densities. This occurrence is completely different from what we observed in benzene,[54] where a rich chemical reactivity was accompained by a strong excimer emission increasing with pressure and reaching its maximum intensity at a pressure near the photochemical threshold pressure. We thus again evidence the strict connection between the increased density and the electronic excitation in the chemical activation of molecular systems. A very weak excimer emission band is observed in indole when the pressure is completely released, likely indicating that excimer formation, like reactivity, occurs at crystal defects.

Acknowledgment. This work has been supported by the European Union under Contract RII3-CT2003-506350, by the Italian Ministero dell'Universitá e della Ricerca Scientifica e Tecnologica (MURST). We wish to thank Paolo Foggi for the useful suggestions and technical support, and Marco De Pas for the collaboration in setting up the electronics of the experiment.

References and Notes

(1) Lautié, A.; Lautié, M. F.; Gruger, A.; Fakhri, S. A. *Spectrochim. Acta* **1980**, *36A*, 85–94.
(2) Suwaiyan, A.; Zwarich, R. *Spectrochim. Acta* **1986**, *42A*, 1017–1020.
(3) Majoube, M.; Vergoten, G. *J. Raman Spectrosc.* **1992**, *23*, 431–444.
(4) Tomkinson, J.; Riesz, J.; Meredith, P.; Parker, S. F. *Chem. Phys.* **2008**, *345*, 230–238.
(5) Roychowdhury, P.; Basak, B. S. *Acta Crystallogr.* **1975**, *B31*, 1559–1563.
(6) Hollas, J. M. *Spectrochim. Acta* **1963**, *19*, 753–767.
(7) Bickel, G. A.; Demmer, D. R.; Outhouse, E. A.; Wallace, S. C. *J. Chem. Phys.* **1989**, *91*, 6013–6019.
(8) Fender, B. J.; Sommeth, D. M.; Callis, P. R. *Chem. Phys. Lett.* **1995**, *239*, 31–37.
(9) Philips, L. A.; Levy, D. H. *J. Chem. Phys.* **1986**, *85*, 1327–1332.
(10) Albinsson, B.; Norden, B. *J. Phys. Chem.* **1992**, *96*, 6204–6212.
(11) Song, P.-S.; Kurtin, W. E. *J. Am. Chem. Soc.* **1969**, *91*, 4892–4906.
(12) Yamamoto, Y.; Tanaka, J. *Bull. Chem. Soc. Jpn.* **1972**, *45*, 1362–1366.
(13) Palit, N. B.; Chakravorty, S. C.; Chaudhuri, M. K. *Spectrochim. Acta* **1979**, *35A*, 701–702.
(14) Andrews, L. J.; Forster, L. S. *Photochem. Photobiol.* **1974**, *19*, 353–360.
(15) Strickland, E. H.; Horwitz, J.; Billups, C. *Biochemistry* **1970**, *9*, 4914–4921.

(16) Lami, H.; Glasser, N. *J. Chem. Phys.* **1986**, *84*, 597–604.
(17) Catalan, J.; Diaz, C. *Chem. Phys. Lett.* **2003**, *368*, 717–723.
(18) Kang, C.; Pratt, D. W. *Int. Rev. Phys. Chem.* **2005**, *24*, 1–36.
(19) Carney, J. R.; Zwier, T. S. *J. Phys. Chem. A* **1999**, *103*, 9943–9957.
(20) Vincent, M.; Gallay, J.; Demchenko, A. P. *J. Phys. Chem.* **1995**, *99*, 14931–14941.
(21) Kang, C.; Timothy, M. K. *J. Chem. Phys.* **2005**, *122*, 174301–8.
(22) Jalviste, E.; Ohta, N. *J. Chem. Phys.* **2004**, *121*, 4730–4739.
(23) Ohrn, A.; Karlstrom, G. *J. Phys. Chem. A* **2007**, *111*, 10468–10477.
(24) Hook, J. W., III; Drickamer, H. G. *J. Chem. Phys.* **1978**, *69*, 811.
(25) Politis, T. G.; Drickamer, H. G. *J. Chem. Phys.* **1981**, *75*, 3203.
(26) Salman, O. A.; Drickamer, H. G. *J. Chem. Phys.* **1982**, *77*, 3329.
(27) Takeuchi, H.; Harada, I. *Spectrochim. Acta* **1986**, *42A*, 1069–1068.
(28) Collier, W. B. *J. Chem. Phys.* **1988**, *12*, 7295–7306.
(29) Callis, P. R. *J. Chem. Phys.* **1991**, *95*, 4230–4240.
(30) Chabalovsky, C. F.; Gamer, D. R.; Jensen, J. O.; Krauss, M. *J. Phys. Chem.* **1993**, *97*, 4608–4613.
(31) Lombardi, J. R. *J. Phys. Chem. A* **1999**, *103*, 6335–6338.
(32) Sobolewski, A. L.; Domcke, W. *Chem. Phys. Lett.* **1999**, *315*, 293–298.
(33) Platt, J. R. *J. Chem. Phys.* **1949**, *17*, 484–495; **1951**, *19*, 101−118.
(34) Klessinger, M.; Michl, J. *Excited States and Photochemistry of Organic Molecules*; VCH Publishers, Inc.: New York, 1995.
(35) Callis, P. R. *Method. Enzymol.* **1997**, *278*, 113–150.
(36) Vivian, J. T.; Callis, P. R. *Biophys. J.* **2001**, *80*, 2093–2109.
(37) Callis, P. R.; Petrenko, A.; Muino, P. L.; Tusell, J. R. *J. Phys. Chem. B* **2007**, *111*, 10335–10339.
(38) Broos, J.; Tveen-Jensen, K.; de Waal, E.; Hesp, B. H.; Jackson, J. B.; Canters, G. W.; Callis, P. R. *Angew. Chem., Int. Ed.* **2007**, *46*, 5137–5139.
(39) Meersman, F.; Dobson, C. M.; Heremans, K. *Chem. Soc. Rev.* **2006**, *35*, 908–917.
(40) Mishra, R.; Winter, R. *Angew. Chem., Int. Ed.* **2008**, *47*, 6518–6521.
(41) Winter, R.; Lopes, D.; Grudzielanek, S.; Vogtt, K. *J. Non-Equilib. Thermodyn.* **2007**, *32*, 41–97.
(42) Hemley, R. J. *Annu. Rev. Phys. Chem.* **2000**, *51*, 763–800.
(43) Schettino, V.; Bini, R.; Ceppatelli, M.; Ciabini, L.; Citroni, M. *Adv. Chem. Phys.* **2005**, *131*, 105–242.
(44) Ciabini, L.; Santoro, M.; Bini, R.; Schettino, V. *J. Chem. Phys.* **2002**, *116*, 2928–2935.
(45) Ciabini, L.; Santoro, M.; Gorelli, F. A.; Bini, R.; Schettino, V.; Raugei, S. *Nat. Mater.* **2007**, *6*, 39–43.
(46) Pruzan, Ph.; Chervin, J. C.; Forgerit, J. P. *J. Chem. Phys.* **1992**, *96*, 761–767.
(47) Ceppatelli, M.; Santoro, M.; Bini, R.; Schettino, V. *J. Chem. Phys.* **2003**, *118*, 1499–1506.
(48) Citroni, M.; Ceppatelli, M.; Bini, R.; Schettino, V. *Science* **2002**, *295*, 2058–2060.
(49) Ciabini, L.; Santoro, M.; Bini, R.; Schettino, V. *Phys. Rev. Lett.* **2002**, *88*, 0855051–0855054.
(50) Santoro, M.; Ceppatelli, M.; Bini, R.; Schettino, V. *J. Chem. Phys.* **2003**, *118*, 8321–8325.
(51) Chelazzi, D.; Ceppatelli, M.; Santoro, M.; Bini, R.; Schettino, V. *Nat. Mater.* **2004**, *3*, 470–475.
(52) Citroni, M.; Ceppatelli, M.; Bini, R.; Schettino, V. *J. Phys. Chem. B* **2007**, *111*, 3910–3917.
(53) Drickamer, H. G.; Frank, C. W.; Slichter, C. P. *Proc. Natl. Acad. Sci.* **1972**, *69*, 933–937.
(54) Citroni, M.; Bini, R.; Foggi, P.; Schettino, V. *Proc. Natl. Acad. Sci.* **2008**, *105*, 7658–7663.
(55) Bini, R.; Ballerini, R.; Pratesi, G.; Jodl, H. J. *Rev. Sci. Instrum.* **1997**, *68*, 3154–3160.
(56) Wilson, E. B. *Phys. Rev.* **1934**, *45*, 706–714.
(57) Lord, R. C.; Miller, F. A. *J. Chem. Phys.* **1942**, *10*, 328–341.
(58) Citroni, M.; Datchi, F.; Bini, R.; Di Vaira, M.; Pruzan, Ph.; Canny, B.; Schettino, V. *J. Phys. Chem. B* **2008**, *112*, 1095–1103.
(59) Schettino, V.; Bini, R.; Cardini, G.; Ceppatelli, M.; Citroni, M.; Pagliai, M. *Nuovo Cimento B* **2009**, *123B*, 1399–1414.
(60) Blais, N. C.; Engelke, R.; Sheffield, S. A. *J. Phys. Chem. A* **1997**, *101*, 8285–8295.
(61) Offen, H. W. *J. Chem. Phys.* **1966**, *44*, 699–703.
(62) Jones, P. F.; Nicol, M. *J. Chem. Phys.* **1968**, *48*, 5440–5447.
(63) Brillante, A.; Della Valle, R. G.; Farina, R.; Venuti, E. *Chem. Phys.* **1995**, *191*, 177–184.
(64) Dreger, Z. A.; Lucas, H.; Gupta, Y. M. *J. Phys. Chem. B* **2003**, *107*, 9268–9274.

JP907169P